PAPER

Check for updates

Interconnected donor–acceptor-additive effects on the microstructure and device performance of PM6 : Y6 solar cells

Edgar Gutiérrez-Fernández,†*[ab] Albert Harillo-Baños,[c] Eduardo Solano, [d]
Oier Bikondoa, [a] Junkal Gutierrez, [e] Agnieszka Tercjak, [e]
Mariano Campoy-Quiles, [c] Sergi Riera-Galindo *[c] and Jaime Martín *[fg]

The microstructure of the donor and acceptor materials within a bulk heterojunction is critical to the performance of organic solar cells, significantly influencing charge generation, transport, and overall efficiency and stability. Here, we studied the role of the donor : acceptor ratio and the use of additives on the resulting microstructure in films and devices based on PM6 : Y6. A detailed study of the resulting structures, mainly by X-ray scattering, indicates that the molecular arrangement leading to higher efficiencies is correlated with the presence of a single, well-mixed phase. In this phase, the diffusion of the Y6 molecules is constrained within the PM6 matrix. Interestingly, this microstructure can be achieved either by tuning the composition or by incorporating a solvent additive. Consequently, either approach can be employed to enhance photovoltaic performance.

Introduction

Organic solar cells (OSCs) based on non-fullerene acceptor (NFA) molecules are one of the most successful research threads in soft condensed matter of the last years.[1] The potential of manufacturing wearable, economical photovoltaic devices with reasonable efficiency and stability[2] explains their success. The efficiency now exceeds the 20% threshold[3,4] after the synthesis of Y-family molecules. Current research in this field is focused on establishing meaningful insights into the

connection between the micro-and nanostructures of the blend and its photovoltaic power conversion efficiency and stability.[5]

Although the photovoltaic system comprises at least two elements, a donor and an acceptor material, the actual relations of the micro and nano-structure of those materials with the photovoltaic performance are elusive. It is imperative to understand their structure as a combination of the effects of the single components and those triggered when the experimental conditions are varied. For the moderately rigid conjugated donor polymer PBDB-T-2F (PM6), we previously introduced a new approach to study its structure,[6] which can be seen as a dense amorphous network with rigid paracrystalline domains. Moreover, we have reported an extensive analysis of the rich polymorphic nature of the acceptor molecule BTP-4F (Y6).[7] PM6 : Y6 is a well-known organic photovoltaic mixture that has been extensively characterised in recent years. Building on our previous studies of these materials individually, we aim to leverage the knowledge gained to better understand their behaviour in photovoltaic blends.

Unsolved questions about the behaviour of the blended microstructure and its relationship with the properties of the device blur the right track to fabricate photovoltaic devices, in which the molecular packing within single and mixed phases is especially important.[8–10] Here, we focus on specific structural features of the blend, inquiring how they are correlated with the device performance.

The actual photovoltaic layer is casted from a mixed solution; the result is what we call a bulk heterojunction (BHJ). During the

[a] *XMaS, The UK CRG Beamline, Department of Physics, University of Warwick, Gibbet Hill Road, Coventry CV4 7AL, UK*

[b] *POLYMAT and Polymer Science and Technology Department, Faculty of Chemistry, University of the Basque Country UPV/EHU, Manuel de Lardizabal 3, Donostia San Sebastián, 20018, Spain*

[c] *Institute of Materials Science of Barcelona ICMAB-CSIC, Campus Universitat Autònoma de Barcelona (UAB), Bellaterra, 08193 Barcelona, Spain. E-mail: sriera@ticmab.es*

[d] *NCD-SWEET beamline, ALBA Synchrotron Light Source, Carrer de la Llum 2-26, 08290 Cerdanyola del Vallès, Spain*

[e] *Group 'Materials + Technologies', Faculty of Engineering Gipuzkoa, University of the Basque Country (UPV/EHU), Plaza Europa 1, 20018 Donostia-San Sebastián, Spain*

[f] *Oportunius Program, Axencia Galega de Innovacion (GAIN), Xunta de Galicia, Galicia, Spain. E-mail: jaime.martin.perez@tudc.es*

[g] *Universidade da Coruña, Campus Industrial de Ferrol, CITENI, Campus de Esteiro S/N 15403, Ferrol, Spain*

† Present address: ESRF, The European Synchrotron, 71 Avenue des Martyrs, Grenoble, France. E-mail: edgar.gutierrez-fernandez@esrf.fr.

formation of the solid layer, liquid–solid transitions are expected. The result is usually a multiphasic system in which pure, mixed, crystalline, and amorphous domains contribute to the generation and extraction of free charges.[11–13]

In addition to the main solvent, it is common to incorporate a low volume ($<$1%) of an additive or dopant,[14] such as ferrocene,[15] graphyne derivatives,[16] 1-chloronaphtalene (CN),[17] or 1-phenyl-nahpthalene (PN)[18] into the solution. As a general rule, we know that additive usually triggers: (1) the separation of phases between components in the blend;[19] and (2) the crystallisation of the purer domains, preferentially those of the acceptor, less reluctant to crystalise than the rigid donor.[20] Focusing on NFA-based solar cells, evidence suggests that the generation of nanometric, crystal-line pure domains is key for its improvement.[21] Recent literature suggests that the presence of CN triggers the crystallisation of Y6[7,12,17] although this effect is not always clearly identified by X-ray diffraction.[16,22] In addition, we detected a common change in the PM6 diffraction pattern that has not yet been reported.

While many studies have focused on structural analysis of single components, it is key important to shed light on how one component influences the other. This is precisely what we present in this document: how the presence of Y6 have a similar effect on the blend as the presence of a solvent additive, and how both experimental conditions lead to a similar bene-ficial scenario. We show how both crystallisation and phase separation of the PM6:Y6[23,24] system are highly dependent on the ratio between the components, and how 1-chloronaphtalene triggers both Y6 crystallisation and phase separation from the PM6 matrix, which, without this additive, forms a single phase with the acceptor molecule.

Results and discussion

The molecular structures of PM6 and Y6, as well as the device architecture, are shown in Fig. 1a and b. The photovoltaic performance of PM6:Y6 solar cells as a function of the donor:-acceptor ratio was consistent with the findings of previous studies (Fig. 1).[22,25] In this study, an inverted device architec-ture was employed to prioritize stability and reproducibility over absolute power conversion efficiency. The primary aim is to derive fundamental insights into the relationship between microstructure and device performance, rather than to achieve record efficiencies. For a single-junction PM6:Y6 solar cell with an inverted architecture, its maximum efficiency is achieved if: (1) Y6 is more abundant than PM6 and (2) a small volume of solvent additive is added.[22,26] Regarding the second point, we can say so far is that a small amount of additive is beneficial, neutral, or at least not critically damaging, depending on the donor: acceptor ratio. All photovoltaic parameters of the tested devices are compiled in the Supplementary Information (Table S1). Power conversion efficiencies exceeding 10% have been achieved, which aligns with the state of the art for inverted PM6:Y6 systems. However, significantly higher values have been reported in the literature using these same materials.[27] We attribute this discre-pancy primarily to the differences in layer thickness optimisation.
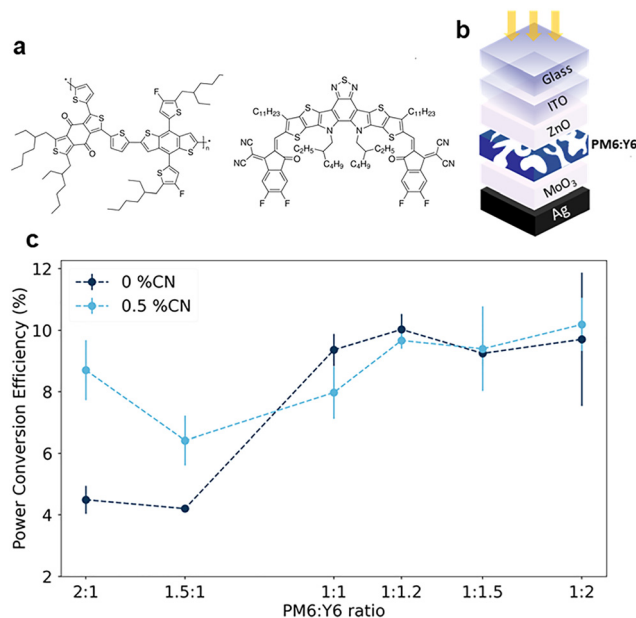

Fig. 1 (a) Chemical structures of PM6 (left) and Y6 (right); (b) inverted architecture of the tested OSCs; (c) average power conversion efficiency values for the tested OSCs. Average values with standard deviation were obtained from at least 3 devices.

Nevertheless, the primary focus of this study is to understand the structural variations induced by changes in the D:A ratio and the addition of the solvent additive. Regarding the short-circuit current (J_{sc}), when there is a higher proportion of PM6, the addition of CN increases the current (up to 20 mA cm^{-2} compared to lower values of approximately 15 mA cm^{-2} without CN). When the donor:acceptor ratio is balanced or there is a higher acceptor content, the values are similar with or without CN, consistently ranging between 20 and 25 mA cm^{-2}. In terms of the fill factor (FF), there are minimal differences, except for the 2:1 ratio, where devices with CN exhibit significantly higher values. No significant differences are observed in the open-circuit voltages (V_{oc}). When the Y6 content increases, the values become even more similar.

In numerous organic photovoltaic systems,[28] research indicates that the ideal device parameters are typically achieved with a donor-to-acceptor ratio of 1:1, with a modest surplus of acceptor material ranging from 1:1.2 to 1:1.6. Under equal mass conditions, a percolated, homogeneous, and bicontinu-ous network is expected to form.[29] A small amount of solvent additive disturbs this network, inducing crystallisation and other diffusion effects that are beneficial. In this study, we use 0.5% volume of CN with respect to the volume of chloro-form. Higher CN concentrations ($>$1%) reduces the solar cell performance after strong crystallisation of Y6, where micro-scopic phase separation could be easily observed by polarised optical microscopy (Fig. S1). In polymer-rich devices, CN enhances the photovoltaic performance, whereas in acceptor-rich devices, the effect appears to be neutral. Herein, we propose a meaningful explanation for the combined effect of the additive and donor:acceptor ratio.
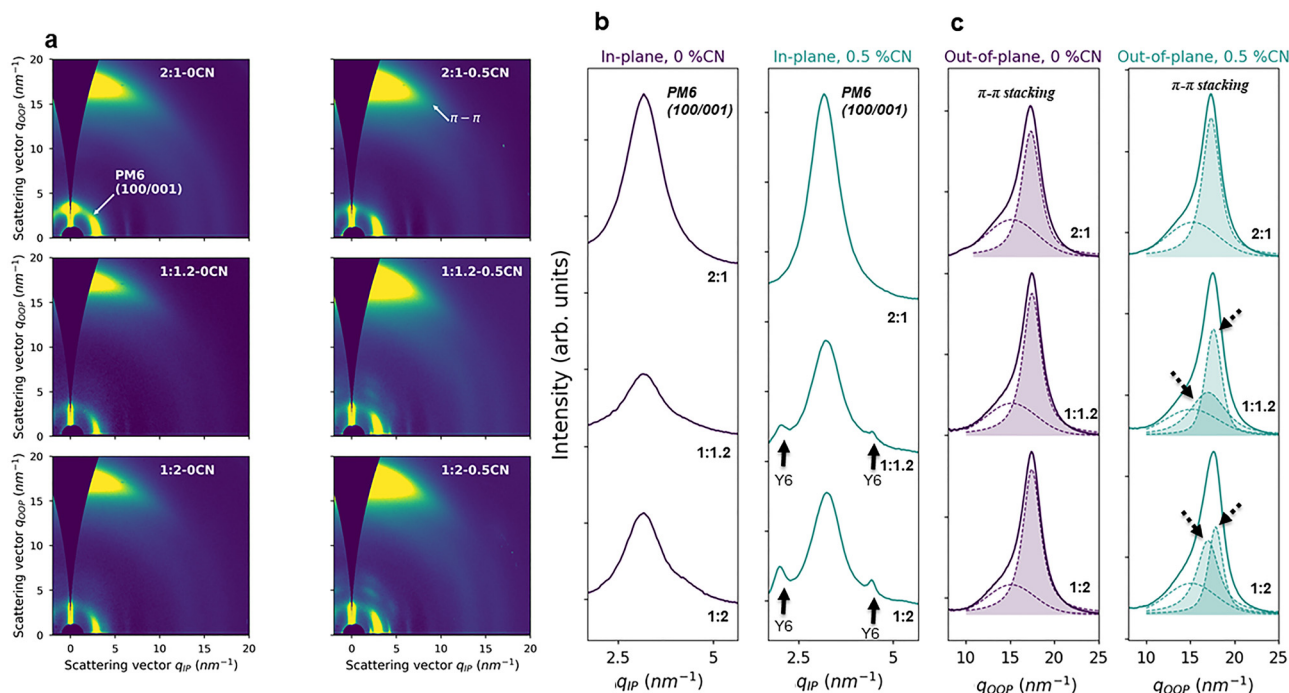
This journal is © The Royal Society of Chemistry 2025

J. Mater. Chem. C, 2025, **13**, 22722–22729 | **22723**

Fig. 2 PM6 : Y6 thin films with different donor:acceptor ratios were deposited from a chloroform solution without (0%) or with (0.5%) 1-chloronaphtalene (CN). (a) 2-D GIWAXS patterns; (b) and (c) integrated profiles on specific regions of the patterns: (b) q_{IP} = 2–6 nm^{-1} along the in-plane axis (centred on the 100/001 PM6 peaks), (c) q_{OOP} = 10–25 nm^{-1} along the out-of-plane axis (centred on the π–π stacking peaks). Both peak regions are highlighted with arrows in the first row of patterns.

Synchrotron Grazing-Incidence Wide-Angle X-ray Scattering (GIWAXS) experiments on thin films helps to cast light on the convoluted structure between PM6 and Y6, revealing insights about crystallinity, molecular orientations, and intermolecular interactions. The entire study is presented in Fig. S2 and S3. The selected patterns are shown in Fig. 2a. For clarity, the azimuthally integrated in-plane and out-of-plane 1D intensity profiles are shown in Fig. 2b and c, respectively.

Several common features are identified. The peaks (100) and (001) are associated to PM6 and close enough between each other at $q \approx 3 \text{nm}^{-1}$. There are two reflections from the Y6 crystals, marked with arrows in Fig. 2b (q = 2.2 and 4.3 nm^{-1}).[7] These Y6 reflections appear only if Y6 is predominant and in the presence of the solvent additive (CN). Both conditions must be fulfilled to detect the crystallisation of Y6. While this crystallisation has been observed in many works,[21] a further analysis of the peak corresponding to the π–π stacking reflection (at $q \approx 17 \text{ nm}^{-1}$)[30] made us identifying a subtle splitting of peaks, only present in the samples where Y6 is partially crystallised (Fig. 2c, the peak splitting is highlighted with dashed arrows). In the remaining cases, where Y6 crystallisation is not detected, the π–π stacking profile is reasonably adjusted with only one peak (see Fig. S4). For every sample, we had to add an additional, ubiquitous peak at $q \sim 15 \text{ nm}^{-1}$, which we associate with the amorphous component of the film. It is important to mention that several factors increase the complexity of performing an accurate peak fitting in grazing incidence data acquired from polymer samples. For example, the disordered nature of the bulk heterojunction and the effect of beam footprint on the

sample contributes to the broadening of the detected peaks. To ensure consistency, data were acquired under equivalent experimental conditions, and an identical fitting approach was applied across all samples. This approach is described in the supplementary document. The quality of the fitting can be assessed by checking Fig. S4, S5 and Tables S2, S3. There is a remarkably increase of the residue (difference between experimental and fitted curve) for Y6-rich samples with CN when fitted with two peaks, that is evidently fixed when a third peak is added. Further analysis was made by calculating the second derivative of the experimental profiles, but the peaks are too convoluted to determine if they contain an additional peak. Nevertheless, the profiles we claim to contain three peaks show a hint of a local minimum, highlighted with arrows (Fig. S6).

Since this difference matches with the Y6-crystallised samples, this observation supports the interpretation that the peak splitting is real, and it is suggesting two structural scenarios for PM6 and Y6. The location of the single or double peak is plotted in Fig. 3a. The q maximum of the single peak is located in between the positions of single Y6 and PM6 samples, while the split peaks are closer to these ones. It is trivial to identify one of the split peaks to the presence pure crystalline domains of Y6. On the other hand, we propose that the single peak is correlated with a unique, well-blended phase of PM6 : Y6, where PM6 and Y6 molecules are homogeneously mixed in a single thermodynamic phase where Y6 diffusion is restricted. If diffusion is restricted, Y6 does not crystallise. To support this idea, we performed GIWAXS experiments while increasing the temperature up to 300 °C to all samples. Two possible scenarios were

22724 | *J. Mater. Chem. C*, 2025, **13**, 22722–22729

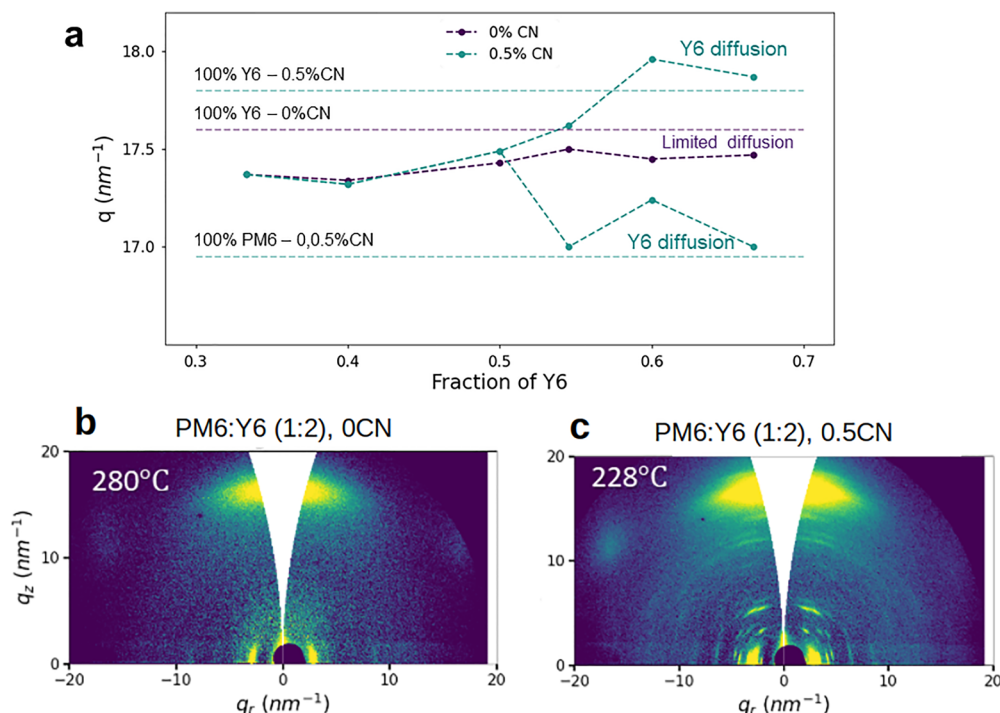This journal is © The Royal Society of Chemistry 2025

Fig. 3 (a) q-position(s) of the $\pi-\pi$ stacking peak(s) maximum from GIWAXS of PM6 : Y6 thin films with different donor:acceptor ratios, deposited from a chloroform solution without (0%) or with (0.5%) 1-chloronaphtalene (CN). The dashed horizontal lines represent the q-positions of this peak for the patterns of the single components PM6 and Y6 (0% and 0.5% CN). (b) and (c) GIWAXS patterns from Y6-rich samples at high temperature, (b) without and (c) with 1-chloronaphtelene.

identified: (i) Y6 crystallizes within the PM6 : Y6 matrix, or (ii) crystallization does not occur (see Fig. 3b and Fig. S7).

The crystallisation onset is around 220 °C, as reported,[7] and the samples in which Y6 crystallises are the ones that show the $\pi-\pi$ stacking peak splitting. In the absence of a solvent additive or for PM6-rich samples, Y6 does not crystallise below 280 °C (Fig. S8). Between 280 °C and 300 °C, the film quickly degrades, possibly due to the chemical decomposition of Y6 in combination with the damage induced by the X-ray beam. Even though we collected data on the non-hit regions of the film and reduced the acquisition time as much as possible, above 280 °C beam damage was always visible. This experiment directly proves that Y6 only crystallizes if the additive (CN) is able to induce partially ordered Y6 regions during the casting of the layer, so these will be present at room temperature. This finding reinforces the idea that, in the samples where no Y6 crystallization is detected, the Y6 is not able to diffuse out of the PM6 matrix and form pure domains, large enough to diffract the X-ray beam. Therefore, together with the previous peak fitting analysis, it supports the idea that a single PM6 : Y6 phase is formed when PM6 is predominant or no additive is added.

The diffusion of Y6 and consequent phase separation between PM6 and Y6 is further supported by atomic force microscope (AFM) and scanning transmission electron microscopy energy dispersive X-ray spectroscopy (STEM-EDS) images in Fig. 4. For PM6-rich blends (2 : 1), the texture of the film does not change after the addition of CN; both surfaces are populated by fiber-like domains, characteristic of PM6 (Fig. S9) and other similar

conjugated polymers.[6,31] The roughness of the Y6-rich samples increases after the addition of CN. The STEM texture also changes and is more evident as Y6 becomes more predominant (1 : 2), further supported by the nitrogen EDS mapping.

Excessive phase separation is usually the cause of the eventual depletion of photovoltaic performance.[32] In this work, inducing phase separation in Y6-rich cells do not clearly enhance their performance (Fig. 1), although this effect is convoluted with Y6 crystallisation. A PM6-rich system, hence a diffusion-restricted PM6 : Y6 phase, experiences a remarkable increase in performance after adding the solvent additive, reaching values close to the maximum of this present work. For PM6-rich samples, CN modifies the PM6 : Y6 structure without inducing Y6 crystallization or phase separation. Recently, Zhang *et al.* highlighted how the presence of CN hinders the crystallisation of PM6 owing to its low solubility.[33] The only structural effect observed in the PM6-rich samples is the reorientation of the (100) PM6 reflection (Fig. 2a). The GIWAXS patterns of the single PM6 samples with CN reveal this effect (Fig. 5).

The presence of CN promotes a ''face-on'' configuration of PM6 molecules, with the $\pi-\pi$ stacking reflection along the vertical (q_z) and (h00) planes along the horizontal (q_r) axis. We want to highlight the rearrangement of the (100) and (300) reflections from the vertical to the horizontal axis (Fig. 5b and c). This is the same effect observed in the pattern when the Y6 content increases (Fig. 2a). Both Y6 and CN induce the reorientation of PM6 molecules, which is beneficial for the performance (Fig. 1c). The nature of the (100) peak oriented in the
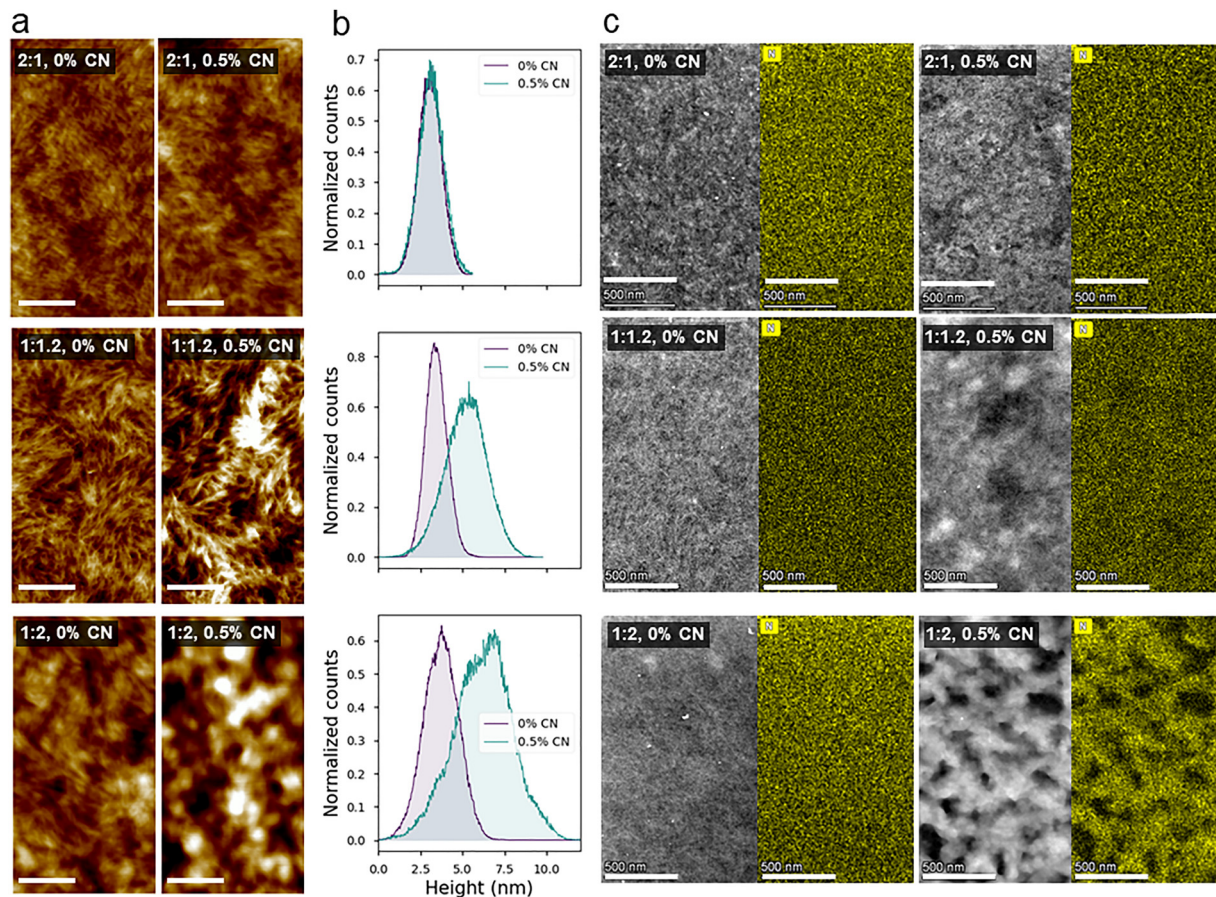
This journal is © The Royal Society of Chemistry 2025

J. Mater. Chem. C, 2025, **13**, 22722–22729 | **22725**

Fig. 4 PM6 : Y6 thin films with different donor:acceptor ratios, deposited from a solution without (0%) or with (0.5%) 1-chloronaphtalene (CN). (a) AFM height images: scale bars are 200 nm, (b) height histograms, (c) STEM-EDS maps, nitrogen-filtered on the right: scale bars are 500 nm.

out-of-plane direction in PBDB-T polymers is related to the presence of self-aggregated structures in the solution.[34] Because the solutions were deposited from chloroform at a relatively low temperature (45 °C), it is reasonable to assume that the single PM6 films and PM6-rich devices contain pre-aggregated clusters. Consequently, the presence of CN and/or Y6 in the solution helps to dilute these PM6 aggregates, either in the solution itself or during film formation. Following this idea, the inclusion of Y6 would contribute to creating a percolated network and diluting the PM6 clusters, promoting a single, well-mixed phase of PM6 : Y6.[35,36] Within this phase, non-crystalline Y6 and non-aggregated PM6 preserve a favourable orientation for the polymer, and the diffusion of the acceptor is restricted. These conditions are consistent with good efficiency values and are promising for their stability.

In order to demonstrate that the rearrangement of the (100) PM6 peak is a collective effect of Y6 and CN, and not because of the dilution effect of chloroform, we characterised diluted PM6 samples by GIWAXS (Fig. S10). As predicted, the pattern from a single diluted PM6 sample still exhibits an intense vertically oriented (100) peak. Further analysis of the PM6 reflections is presented in Fig. S11 and Table S4. The fact that CN is also affecting the aggregation and the configuration of PM6 is further supported by AFM (Fig. S12) and UV-vis absorption

spectroscopy (Fig. S13) experiments, respectively. The AFM images reveals changes in surface texture consistent with different aggregation states, showing a clear increase of the size of PM6 aggregates upon the addition of CN. On the other hand, the redshift of the lowest energy transition peak (0–0 vibronic), at least from a first analysis, points to an increase of the effective backbone conjugation length.[37] Correlating these effects with photovoltaic performance is a complex task. The solar cell efficiency joints many other different effects that are not taking place in the active layer and, of course, effects that cannot be captured by X-rays. Nevertheless, the aim of this study is to find a consistent structural scheme by changing only two parameters (donor:acceptor ratio and solvent additive). We have shown that the optimal performance of the PM6 : Y6 system coincides with a well-mixed phase, without visible Y6 crystalline domains and without self-aggregated PM6 clusters from the solution.

Finally, we speculate on the relationship between phase separation and device stability. A high diffusion coefficient of the acceptor molecules is correlated with lower device stability.[2] In this work, we demonstrate how, in the same photovoltaic system, the diffusion of acceptor molecules is extremely dependent on the donor:acceptor ratio and the incorporation of a solvent additive. Accordingly, a system with a blended phase of PM6 : Y6 (e.g. 1 : 1.2-0CN) is likely to present higher

22726 | J. Mater. Chem. C, 2025, **13**, 22722–22729

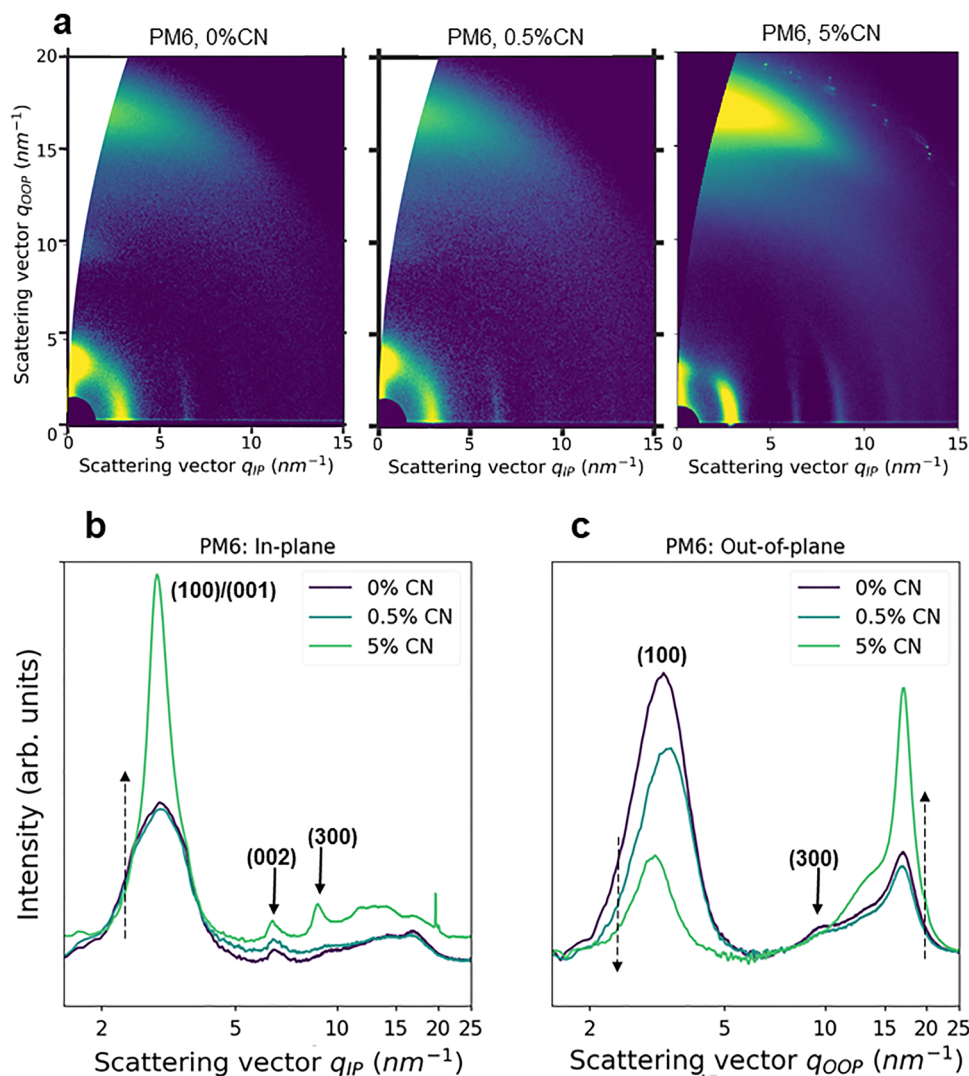This journal is © The Royal Society of Chemistry 2025

Fig. 5 PM6 thin films deposited from a chloroform solution with different volume percentages of 1-chloronaphtalene: (a) 2D GIWAXS patterns, (b) and (c) intensity profiles after azimuthal integration along the q_{IP} (in-plane) (b) and q_{OOP} (out-of-plane) axes (c).

thermodynamic stability than a system with a pure crystalline phase (for example, 1:1.2-0.5CN).

Conclusions

In this work, we established a consistent structural framework to support the photovoltaic performance of PM6:Y6 systems, considering the reciprocal effect between the components and the effect of the solvent additive 1-chloronaphtalene (CN). We show how the maximum performance is likely connected to a single, homogeneous phase of PM6:Y6, in which crystallisation is restricted. When both components are balanced, the use of CN proves more detrimental than beneficial, affecting not only performance but also device stability, as the results indicate that a thermodynamically stable blend is formed when CN is avoided. While this study is fully focused on PM6:Y6, we hope our findings about the coupling effects of the acceptor and the additive in the polymer can be transferred, and will motivate further research on

other similar systems containing D18, PBDBT-2Cl or N3, to name a few. We expect, as well, to see an equivalent effect of CN with other additives, like diiodooctane (DIO) or 1-phenylnaphtalene (PN). Furthermore, the correlations between structure and performance observed in this work are expected to hold for conventional PM6: Y6 devices, as these trends are primarily governed by bulk morphology rather than the specific electrode configuration, thus supporting the generality of our conclusions beyond the inverted architecture employed here.

Conflicts of interest

There are no conflicts to declare.

Data availability

The data that support the findings of this study are available from the corresponding author upon reasonable request.

This journal is © The Royal Society of Chemistry 2025

J. Mater. Chem. C, 2025, **13**, 22722–22729 | **22727**

References

1 S. Shoaee, H. M. Luong, J. Song, Y. Zou, T.-Q. Nguyen and D. Neher, "What we have learnt from PM6: Y6", *Adv. Mater.*, 2024, **36**(20), 2302005.

2 Y. Cui, Y. Xu, H. Yao, P. Bi, L. Hong, J. Zhang, Y. Zu, T. Zhang, J. Qin, J. Ren, Z. Chen, C. He, X. Hao, Z. Wei and J. Hou, "Single-Junction Organic Photovoltaic Cell with 19% Efficiency", *Adv. Mater.*, 2021, **33**(41), 2102420.

3 J. Fu, Q. Yang, P. Huang, S. Chung, K. Cho, Z. Kan, H. Liu, X. Lu, Y. Lang and H. Lai, "Rational molecular and device design enables organic solar cells approaching 20% efficiency", *Nat. Commun.*, 2024, **15**(1), 1830.

4 Y. Y. Jiang, F. Liu and X. Z. Zhu, "Single-junction organic solar cells with a power conversion efficiency of more than 20%", *Nat. Energy*, 2024, **9**(8), 930–931.

5 P. Ding, D. Yang, S. Yang and Z. Ge, "Stability of organic solar cells: toward commercial applications", *Chem. Soc. Rev.*, 2024, **53**(5), 2350–2387.

6 S. Marina, E. Gutierrez-Fernandez, J. Gutierrez, M. Gobbi, N. Ramos, E. Solano, J. Rech, W. You, L. Hueso, A. Tercjak, H. Ade and J. Martin, "Semi-paracrystallinity in semiconducting polymers", *Mater. Horiz.*, 2022, **9**(4), 1196–1206.

7 E. Gutierrez-Fernandez, A. D. Scaccabarozzi, A. Basu, E. Solano, T. D. Anthopoulos and J. Martín, "Y6 Organic Thin-Film Transistors with Electron Mobilities of 2.4 cm2 V−1 s−1 via Microstructural Tuning", *Adv. Sci.*, 2022, **9**(1), 2104977.

8 M. Ghasemi, N. Balar, Z. Peng, H. Hu, Y. Qin, T. Kim, J. J. Rech, M. Bidwell, W. Mask, I. McCulloch, W. You, A. Amassian, C. Risko, B. T. O'Connor and H. Ade, "A molecular interaction–diffusion framework for predicting organic solar cell stability", *Nat. Mater.*, 2021, **20**(4), 525–532.

9 G. Kupgan, X. K. Chen and J. L. Brédas, "Molecular packing of non-fullerene acceptors for organic solar cells: Distinctive local morphology in Y6 vs. ITIC derivatives", *Mater. Today Adv.*, 2021, **11**, 1–25.

10 S. Marina, A. D. Scaccabarozzi, E. Gutierrez-Fernandez, E. Solano, A. Khirbat, L. Ciammaruchi, A. Iturrospe, A. Balzer, L. Yu, E. Gabirondo, X. Monnier, H. Sardon, T. D. Anthopoulos, M. Caironi, M. Campoy-Quiles, C. Müller, D. Cangialosi, N. Stingelin and J. Martin, "Polymorphism in Non-Fullerene Acceptors Based on Indacenodithienothiophene", *Adv. Funct. Mater.*, 2021, **31**(29), 2103784.

11 J. Mai, Y. Xiao, G. Zhou, J. Wang, J. Zhu, N. Zhao, X. Zhan and X. Lu, "Hidden structure ordering along backbone of fused-ring electron acceptors enhanced by ternary bulk heterojunction", *Adv. Mater.*, 2018, **30**(34), 1–8.

12 L. Zhu, M. Zhang, G. Zhou, T. Hao, J. Xu, J. Wang, C. Qiu, N. Prine, J. Ali, W. Feng, X. Gu, Z. Ma, Z. Tang, H. Zhu, L. Ying, Y. Zhang and F. Liu, "Efficient Organic Solar Cell with 16.88% Efficiency Enabled by Refined Acceptor Crystallization and Morphology with Improved Charge Transfer and Transport Properties", *Adv. Energy Mater.*, 2020, **10**(18), 1904234.

13 H. Lai, Q. Zhao, Z. Chen, H. Chen, P. Chao, Y. Zhu, Y. Lang, N. Zhen, D. Mo, Y. Zhang and F. He, "Trifluoromethylation Enables a 3D Interpenetrated Low-Band-Gap Acceptor for Efficient Organic Solar Cells", *Joule*, 2020, **4**(3), 688–700.

14 Y. Lin, Y. Firdaus, M. I. Nugraha, F. Liu, S. Karuthedath, A. H. Emwas, W. Zhang, A. Seitkhan, M. Neophytou, H. Faber, E. Yengel, I. McCulloch, L. Tsetseris, F. Laquai and T. D. Anthopoulos, "17.1% Efficient Single-Junction Organic Solar Cells Enabled by n-Type Doping of the Bulk-Heterojunction", *Adv. Sci.*, 2020, **7**(7), 1–9.

15 L. Ye, Y. Cai, C. Li, L. Zhu, J. Xu, K. Weng, K. Zhang, M. Huang, M. Zeng, T. Li, E. Zhou, S. Tan, X. Hao, Y. Yi, F. Liu, Z. Wang, X. Zhan and Y. Sun, "Ferrocene as a highly volatile solid additive in non-fullerene organic solar cells with enhanced photovoltaic performance", *Energy Environ. Sci.*, 2020, **13**(12), 5117–5125.

16 L. Liu, Y. Kan, K. Gao, J. Wang, M. Zhao, H. Chen, C. Zhao, T. Jiu, A. K. Y. Jen and Y. Li, "Graphdiyne Derivative as Multifunctional Solid Additive in Binary Organic Solar Cells with 17.3% Efficiency and High Reproductivity", *Adv. Mater.*, 2020, **32**(11), 1–7.

17 S. M. Hosseini, N. Tokmoldin, Y. W. Lee, Y. Zou, H. Y. Woo, D. Neher and S. Shoaee, "Putting Order into PM6:Y6 Solar Cells to Reduce the Langevin Recombination in 400 nm Thick Junction", *Sol. RRL*, 2020, **4**(11), 1–7.

18 L. Ye, Y. Xiong, M. Zhang, X. Guo, H. Guan, Y. Zou and H. Ade, "Enhanced efficiency in nonfullerene organic solar cells by tuning molecular order and domain characteristics", *Nano Energy*, 2020, **77**, 105310.

19 X. He, C. C. S. Chan, J. Kim, H. Liu, C.-J. Su, U.-S. Jeng, H. Su, X. Lu, K. S. Wong and W. C. H. Choy, "1-Chloronaphthalene-Induced Donor/Acceptor Vertical Distribution and Carrier Dynamics Changes in Nonfullerene

22728 | *J. Mater. Chem. C*, 2025, **13**, 22722–22729

This journal is © The Royal Society of Chemistry 2025

Organic Solar Cells and the Governed Mechanism'', *Small Methods*, 2022, **6**(3), 2101475.

20 O. Alqahtani, J. Lv, T. Xu, V. Murcia, T. Ferron, T. McAfee, D. Grabner, T. Duan and B. A. Collins, ''High Sensitivity of Non-Fullerene Organic Solar Cells Morphology and Performance to a Processing Additive'', *Small*, 2022, **18**(23), 2202411.

21 W. Zhu, A. P. Spencer, S. Mukherjee, J. M. Alzola, V. K. Sangwan, S. H. Amsterdam, S. M. Swick, L. O. Jones, M. C. Heiber, A. A. Herzing, G. Li, C. L. Stern, D. M. DeLongchamp, K. L. Kohlstedt, M. C. Hersam, G. C. Schatz, M. R. Wasielewski, L. X. Chen, A. Facchetti and T. J. Marks, ''Crystallography, Morphology, Electronic Structure, and Transport in Non-Fullerene/Non-Indacenodithienothiophene Polymer:Y6 Solar Cells, *J. Am. Chem. Soc.*, 2020, **142**(34), 14532–14547.

22 J. Yuan, Y. Zhang, L. Zhou, G. Zhang, H. L. Yip, T. K. Lau, X. Lu, C. Zhu, H. Peng, P. A. Johnson, M. Leclerc, Y. Cao, J. Ulanski, Y. Li and Y. Zou, ''Single-Junction Organic Solar Cell with over 15% Efficiency Using Fused-Ring Acceptor with Electron-Deficient Core'', *Joule*, 2019, **3**(4), 1140–1151.

23 Z. C. Wen, H. Yin and X. T. Hao, ''Recent progress of PM6:Y6-based high efficiency organic solar cells'', *Surf. Interfaces*, 2021, **23**, 100921.

24 Q. Guo, Q. Guo, Y. Geng, A. Tang, M. Zhang, M. Du, X. Sun and E. Zhou, ''Recent advances in PM6:Y6-based organic solar cells'', *Mater. Chem. Front.*, 2021, **5**(8), 3257–3280.

25 K. Nakano, K. Terado, Y. Kaji, H. Yoshida and K. Tajima, ''Reduction of Electric Current Loss by Aggregation-Induced Molecular Alignment of a Non-Fullerene Acceptor in Organic Photovoltaics'', *ACS Appl. Mater. Interfaces*, 2021, **13**(50), 60299–60305.

26 P. Wan, X. Chen, Q. Liu, S. Mahadevan, M. Guo, J. Qiu, X. Sun, S. W. Tsang, M. Zhang, Y. Li and S. Chen, ''Direct Observation of the Charge Transfer States from a Non-Fullerene Organic Solar Cell with a Small Driving Force'', *J. Phys. Chem. Lett.*, 2021, **12**(43), 10595–10602.

27 X. Yang, B. Li, X. Zhang, S. Li, Q. Zhang, L. Yuan, D.-H. Ko, W. Ma and J. Yuan, ''Intrinsic Role of Volatile Solid Additive in High-Efficiency PM6:Y6 Series Nonfullerene Solar Cells'', *Adv. Mater.*, 2023, **35**(24), 2301604.

28 Z. Wang, Z. Peng, Z. Xiao, D. Seyitliyev, K. Gundogdu, L. Ding and H. Ade, ''Thermodynamic properties and molecular packing explain performance and processing procedures of three D18: NFA organic solar cells'', *Adv. Mater.*, 2020, **32**(49), 2005386.

29 N. Yao, J. Wang, Z. Chen, Q. Bian, Y. Xia, R. Zhang, J. Zhang, L. Qin, H. Zhu, Y. Zhang and F. Zhang, ''Efficient Charge Transport Enables High Efficiency in Dilute Donor Organic Solar Cells'', *J. Phys. Chem. Lett.*, 2021, **12**(20), 5039–5044.

30 R. Noriega, J. Rivnay, K. Vandewal, F. P. V. Koch, N. Stingelin, P. Smith, M. F. Toney and A. Salleo, ''A general relationship between disorder, aggregation and charge transport in conjugated polymers'', *Nat. Mater.*, 2013, **12**(11), 1038–1044.

31 S. Zhang, Y. Qin, J. Zhu and J. Hou, ''Over 14% Efficiency in Polymer Solar Cells Enabled by a Chlorinated Polymer Donor'', *Adv. Mater.*, 2018, **30**(20), 1–7.

32 J. Xue, H. B. Naveed, H. Zhao, B. Lin, Y. Wang, Q. Zhu, B. Wu, Z. Bi, X. Zhou and C. Zhao, ''Kinetic processes of phase separation and aggregation behaviors in slot-die processed high efficiency Y6-based organic solar cells'', *J. Mater. Chem. A*, 2022, **10**(25), 13439–13447.

33 J. Zhang, Z. Li, X. Jiang, L. Xie, G. Pan, A. Buyan-Arivjikh, T. Baier, S. Tu, L. Li, M. Schwartzkopf, S. K. Vayalil, S. V. Roth, Z. Ge and P. Müller-Buschbaum, ''Revealing the Effect of Solvent Additive Selectivity on Morphology and Formation Kinetics in Printed Non-fullerene Organic Solar Cells at Ambient Conditions'', *Adv. Energy Mater.*, 2025, **15**(17), 2404724.

34 B. Du, R. Geng, W. Tan, Y. Mao, D. Li, X. Zhang, D. Liu, W. Tang, W. Huang and T. Wang, ''Heating induced aggregation in non-fullerene organic solar cells towards high performance'', *J. Energy Chem.*, 2021, **54**, 131–137.

35 H. Sirringhaus, P. J. Brown, R. H. Friend, M. M. Nielsen, K. Bechgaard, B. M. W. Langeveld-Voss, A. J. H. Spiering, R. A. J. Janssen, E. W. Meijer, P. Herwig and D. M. D. Leeuw, ''Two-dimensional charge transport in self-organized, high-mobility conjugated polymers'', *Nature*, 1999, **401**(6754), 685–688.

36 H. Zhao, H. B. Naveed, B. Lin, X. Zhou, J. Yuan, K. Zhou, H. Wu, R. Guo, M. A. Scheel, A. Chumakov, S. V. Roth, Z. Tang, P. Müller-Buschbaum and W. Ma, ''Hot Hydrocarbon-Solvent Slot-Die Coating Enables High-Efficiency Organic Solar Cells with Temperature-Dependent Aggregation Behavior'', *Adv. Mater.*, 2020, **32**(39), 1–10.

37 R. Harris, C.-Y. Chang, J. Guo, H. Ivov Gonev and T. M. Clarke, ''Modulating Polaron Behavior in PM6 Blends with Nonfullerene and Fullerene Acceptors: the Importance of Singlet Energy Transfer'', *Adv. Mater. Interfaces*, 2025, **12**(14), 2400779.

This journal is © The Royal Society of Chemistry 2025

J. Mater. Chem. C, 2025, **13**, 22722–22729 | **22729**